Genes & Diseases (2024) 11, 397–412

Available online at www.sciencedirect.com

ScienceDirect

journal homepage: www.keaipublishing.com/en/journals/genes-diseases

FULL LENGTH ARTICLE

Overcoming adaptive resistance in AML by synergistically targeting FOXO3A-GNG7-mTOR axis with FOXO3A inhibitor Gardenoside and rapamycin

Zhe Chen [a,b,1], Qian Guo [c,1], Shichen Huang [d], Lei Li [a], Feng Wu [b], Zhilong Liu [a], Zhigang Li [b], Tao Chen [a], Guanbin Song [c], Shuangnian Xu [a,*], Jieping Chen [a,*], Yu Hou [b,*,#]

[a] *Department of Hematology, Southwest Hospital, Third Military Medical University (Army Medical University), Chongqing 400038, China*
[b] *Institute of Life Sciences, Chongqing Medical University, Chongqing 400016, China*
[c] *Key Laboratory of Biorheological Science and Technology, Ministry of Education, College of Bioengineering, Chongqing University, Chongqing 400044, China*
[d] *Chongqing Foreign Language School, Chongqing 400039, China*

Received 4 November 2022; accepted 2 January 2023
Available online 25 January 2023

KEYWORDS
AML;
Combinatorial inhibition;
FOXO3A;
GNG7;
mTOR

Abstract Therapeutic targeting FOXO3A (a forkhead transcription factor) represents a promising strategy to suppress acute myeloid leukemia (AML). However, the effective inhibitors that target FOXO3A are lacking and the adaptive response signaling weakens the cytotoxic effect of *FOXO3A* depletion on AML cells. Here, we show that *FOXO3A* deficiency induces a compensatory response involved in the reactive activation of mTOR that leads to signaling rebound and adaptive resistance. Mitochondrial metabolism acts downstream of mTOR to provoke activation of JNK/c-JUN via reactive oxygen species (ROS). At the molecular level, FOXO3A directly binds to the promoter of *G* protein gamma subunit 7 (GNG7) and preserves its expression, while GNG7 interacts with mTOR and restricts phosphorylated activation of mTOR. Consequently, combinatorial inhibition of FOXO3A and mTOR show a synergistic cytotoxic effect on AML cells and prolongs survival in a mouse model of AML. Through a structure-based virtual screening, we report one potent small-molecule FOXO3A inhibitor (Gardenoside) that exhibits a strong

* Corresponding author.
E-mail addresses: xushuangnian@tmmu.edu.cn (S. Xu), chenjpxn@163.com (J. Chen), houyu@cqmu.edu.cn (Y. Hou).
Peer review under responsibility of Chongqing Medical University.
[1] These authors contributed equally.
[#] Lead contact.

https://doi.org/10.1016/j.gendis.2023.01.002

effect of anti-FOXO3A DNA binding. Gardenoside synergizes with rapamycin to substantially reduce tumor burden and extend survival in AML patient-derived xenograft model. These results demonstrate that mTOR can mediate adaptive resistance to FOXO3A inhibition and validate a combinatorial approach for treating AML.

Introduction

Acute myeloid leukemia (AML) is an aggressive blood malignancy characterized by the accumulation of myeloid progenitor cells with uncontrolled proliferation and impaired differentiation.[1] Accumulating evidence indicates that AML cells are preserved by a multilevel regulatory network, including cell cycle regulators, transcription factors, kinase-related factors, epigenetic factors, cytokines, and niche cells.[2,3] These intracellular and niche factors synergistically accelerate AML progression and cause chemotherapy resistance, resulting in poor outcomes and survival of AML patients.[1,4] Thus, elucidating the molecular networks that maintain leukemia cells will expand the understanding of AML and be beneficial for therapeutic intervention.

Forkhead box O3 (FOXO3), also named FOXO3A, belongs to the Forkhead box family that consists of an evolutionarily conserved group of transcription factors.[5] FOXO3A contains a forkhead winged helix-turn-helix domain (FKH), which is responsible for FOXO3A binding DNA and regulating gene expression.[6] FOXO3A regulates multiple biological processes involved in proliferation, differentiation, apoptosis, and autophagy.[7,8] Importantly, it has been revealed that FOXO3A plays a critical role in leukemia transformation and progression. FOXO3A shows high expression in leukemia-granulocyte macrophage progenitor (L-GMP) compared with GMP.[9] A high FOXO3A level is an adverse prognostic marker and is associated with a poorer prognosis in AML.[10,11] It has been demonstrated that FOXO3A protects *MLL-AF9* leukemia cells from DNA damage and inhibits myeloid maturation, while loss of *FOXO3A* induces myeloid differentiation and attenuates the expansion of AML cells.[9,12] Although treating AML by FOXO3A inhibition shows potential, the pharmacological inhibition of FOXO3A lacks effective inhibitors.

Abundant efforts have been made to identify key oncoproteins in leukemia; nevertheless, single-agent targeted therapies show limited toxicity, and the acquired resistance further limits intervention efficacy.[13] On this basis, drug combinations show promising potential in leukemia treatment, which have the potential to overcome resistance, enhance the cytotoxic effect, and expand the range of treatment.[13–15] For instance, synergistic inhibition of Bcl2 and Bruton's tyrosine kinase abrogates the expansion of diffuse large B-cell lymphoma (DLBCL).[14] A phase III trial has demonstrated that ibrutinib addition is superior to single R–CHOP chemotherapy in a subpopulation of DLBCL.[15] FLT3-internal tandem duplication (FLT-ITD) is a prevalent mutation in AML; compared with single treatment of FLTs tyrosine kinase inhibitors (TKIs), several combinatorial therapies show outstandingly killing efficiency against AML, including Notch inhibitor with TKIs, β-catenin inhibitor with TKIs, and retinoic acid with TKIs.[1,16–18] Previous findings show that *FOXO3A* deficiency inversely activates JNK/c-JUN signaling that weakens the cytotoxic effect of *FOXO3A* depletion on AML cells,[9] suggesting that a combinatorial strategy may enhance the response of AML cells to FOXO3A inhibition. Here, we found that *FOXO3A* deficiency triggered apoptosis and differentiation of AML cells, but also induced activation of mTOR signaling. Pharmacological inhibition of mTOR cooperated with *FOXO3A* depletion to induce AML cell death. Further, we uncovered that FOXO3A transcriptionally regulated the expression of multiple genes related to AML progression, and demonstrated that the target GNG7 (G protein gamma subunit 7) mediated the inhibitory effect of FOXO3A on mTOR via GNG7/mTOR interaction. Moreover, we screened a small molecule, Gardenoside, which interacted with the helix domain of FOXO3A protein to impede the function of FOXO3A. The combinatorial use of Gardenoside and rapamycin (an mTOR inhibitor) substantially delayed AML progression compared with single-agent treatments, providing a combinatorial approach for treating AML.

Materials and methods

Mice

C57BL/6J mice and NOD/SCID mice were purchased from Beijing Sibeifu Science (China). All mice were maintained in the Animal Center of Army Medical University. The experiments used 8-to-10-week-old mice (both male and female) and were approved by the Animal Committee of the Institute of Zoology, Army Medical University.

Cell culture

The human AML cell lines, THP-1, U-937, and HL-60 were obtained from America Type Culture Collection (ATCC) and cultured in RPMI1640 with 15% fetal bovine serum (FBS) (Gibico) and 1% penicillin/streptomycin (Hyclone). HEK293T cells were cultured in DMEM containing 10% FBS and 1% penicillin/streptomycin. Primary AML patient cells were cultured in IMDM supplemented with 20% FBS, 1% penicillin/streptomycin, and 10 ng/mL human cytokines TPO, SCF, FLT3L, IL-3, and IL-6 (StemCell Technologies). The use of patient cells was approved by the institutional review board of Army Medical University. For drug treatment, rapamycin (100 nM, Selleck), SP600125 (5 μM, Selleck), acetylcysteine

(2 mM, Selleck), or Gardenoside (5 μM, TargetMol) were added to the medium for indicated days.

Plasmids and lentivirus production

To generate the vectors for specific knockout of *FOXO3A* and *GNG7*, sgRNAs of target genes were designed on the CRISPOR website (http://crispor.tefor.net/crispor.py) (Table S1) and cloned into vector lentiCRISPR-V2. To generate the vectors for the expression of CDKN2D-specific shRNA, we designed the sequence of shRNAs and cloned shRNAs into the vector pLKO.1-EGFP-puro (primer sequences; Table S1). To generate the vectors of GNG7 expression, we amplified transcriptional regions by RT-PCR and cloned the regions into a pCDH-puro vector (Table S1). The pLV-FOXO3A plasmid was purchased from Cyagen and the MIGR1-MLL-AF9 plasmid was a gift from Dr. Haitao Bai. For lentivirus production, 293T cells were transfected with an interesting vector combined with pMD2. G and psPAX2. For retrovirus production, 293T cells were transfected with MIGR1-MLL-AF9-GFP plasmid combined with pCL-ECO. The medium was replaced with fresh medium at 12 h after transfection and culture supernatants were collected at 48 h and 72 h. The virus was stored at −80 °C until use. Positively infected cells were isolated using flow cytometry sorting (GFP) or puromycin treatment.

AML cell line-derived xenograft and PDX model

For xenograft mice, 1×10^6 U-937 cells were transplanted into the sub-lethally irradiated (2 Gy) NOD/SCID mice intravenously. After 10 days of transplantation, mice were treated with vehicle, rapamycin (4 mg/kg, i. p. injection; three times a week), SP600125 (15 mg/kg, i. p. injection; three times a week), or combination (rapamycin plus SP600125) for three weeks. To generate the patient-derived tumor xenograft (PDX) mouse model, 1×10^6 AML patient-derived bone marrow (BM) mononuclear cells were transplanted into the sub-lethally irradiated (2 Gy) NOD/SCID mice intravenously, and drug treatment was started 10 days later. Gardenoside (15 mg/kg) and rapamycin (4 mg/kg) were administered through intraperitoneal injection. Both Gardenoside and rapamycin were injected three times a week for a total of three weeks. All experiments involving human samples were approved by the Medical Ethics Committees of Southwest Hospital.

Murine *MLL-AF9* leukemia model

MLL-AF9 mice were generated following the protocol of previous work.[19] Briefly, wild-type C57BL/6 J mice were treated with a dose of 150 mg/kg 5-Fu (Sigma−Aldrich) via intraperitoneal injection and were sacrificed 5 days later. BM cells (hematopoietic stem/progenitor cells enriched) were collected and infected with *MLL-AF9* retrovirus twice in the presence of mouse cytokines (10 ng/mL IL-3, 10 ng/mL IL-6, 20 ng/mL SCF; StemCell Technologies) and 8 mg/mL polybrene (Sigma−Aldrich). Infected cells were transplanted into sub-lethally irradiated (7 Gy) C57BL/6 J mice plus 1×10^6 BM cells (freshly isolated from C57BL/6 J mice) via tail vein injection. When the mice developed full-down AML, primary leukemic BM cells (GFP^+) were collected and sorted by flow cytometry. The leukemia cells were transduced with CRISPR-sgFoxO3a lentivirus and then injected into sub-lethally irradiated (7 Gy) C57BL/6 J mice with 1×10^6 BM cells via tail vein injection. Ten days after transplantation, mice were treated with rapamycin (4 mg/kg, i. p. injection; three times a week), SP600125 (15 mg/kg, i. p. injection; three times a week), or combination (rapamycin plus SP600125) for three weeks.

Cell proliferation and colony-forming assay

To assess the cell proliferation/growth, 2500 cells were seeded into a 96-well plate in triplicates. At indicated time points, cell expansion was assessed by number count or using the Cell Count Kit-8 kit (Beyotime) according to the manufacturer's instructions. For the colony-forming assay, about 10,000 AML patient BM cells or 5000 AML cells (THP-1, U-937, and HL-60) were plated in 35-mm tissue culture dishes containing methylcellulose medium (MethoCult H4434, StemCell Technologies) according to the manufacturer's instructions.

Flow cytometry analysis

Human leukemia cells in peripheral blood, spleen, and BM were analyzed using PE-anti-human CD45 antibody (BioLegend). APC-anti-human CD11b (BioLegend) was used for myeloid maturation analysis. For the detection of mTOR activity, the cells were stained with anti-p-mTOR (BioLegend) or anti-p-S6 (BioLegend) and then incubated with FITC-anti-mouse antibody (BioLegend). The PE-anti-PThe FITC Annexin V Apoptosis Detection Kit with PI (BioLegend) was used for apoptosis analysis. Mito-Tracker Red CMXRos (Beyotime) was used for mitochondrial staining. Reactive Oxygen Species Assay Kit (Beyotime) was used for ROS measurement. All cells were analyzed by Flow cytometry on BD FACSCanto II and all data were analyzed by FlowJo software.

Mitochondrial DNA quantification and ATP measurement

Total DNA was isolated from 100,0000 cultured AML cells using Hipure Tissue DNA Mini Kit (Magen) according to the manufacturer's instructions. Mitochondrial DNA was analyzed by quantitative PCR (Table S1). The cellular ATP level was detected using the Enhanced ATP Assay Kit (Beyotime) according to the manufacturer's instructions.

Quantitative RT-PCR and ChIP-PCR

The quantitative RT-PCR was performed as described previously.[20] Briefly, total RNA was isolated using the Total RNA Isolation Kit (Thermo Fisher) according to the manufacturer's instructions. cDNA was reverse-transcribed using PrimeScript RT reagent Kit (Takara) and subjected to real-time PCR with SYBR Green Supermix (Bio-Rad) in an iCycler iQ Real Time PCR Detection System (Bio-rad). All primers are listed in Table S1. All samples were run in triplicate. GAPDH was used as an internal control for mRNA.

ChIP assays were performed using EZ-ChIP Chromatin Immunoprecipitation Kit (Milipore). In brief, the cells were fixed with 1% formaldehyde for 10 min, and the fixation reaction was quenched with glycine to a final concentration of 125 mM. The cells were lysed and sonicated until the desired lengths were achieved (100—500 bp). Then, 5 μg of anti-FOXO3A (#12829, Cell Signaling Technology) or control IgG were used for immunoprecipitation. After the elution of DNA from precipitated immunocomplexes, quantitative real-time PCR was performed with specific primers (Table S1).

Western blot and immunoprecipitation assay

For Western blot, AML cells were extracted in RIPA lysis buffer (Beyotime). Protein extracts were separated by SDS-PAGE. The antibodies used in this study were against the following: FOXO3A (1:1000; #12819; Cell Signaling Technology), p-mTOR (1:500; 610,301; BioLegend), mTOR (1:500; 20657-1-AP; Proteintech), mTOR (1:2500; 66888-1-Ig; Proteintech); S6 (1:1000; AF0258; Beyotime), p-S6 (1:1000; AF5899; Beyotime), JNK1/2/3 (1:1000; AF1048; Beyotime), p-JNK1/2/3 (1:1000; AF1762; Beyotime), C-JUN (1:1000; AF1612; Beyotime), p-C-JUN (1:1000; AF5779; Beyotime), GNG7 (1:1000; A62678-020; EpiGentek), and Tubulin (1:1000; AF0001; Beyotime). Immunoprecipitates were analyzed by Western blot according to standard procedures.

Duolink proximity ligation assay

Duolink proximity ligation assay (PLA) was performed using Duolink *In Situ* Red Starter Kit (Sigma-Aldrich) according to the manufacturer's instructions. Briefly, U-937 cells were plated onto poly-lysine-coated coverslips and then fixed in 4% paraformaldehyde for 20 min. Cells were then permeabilized in Triton X-100 (0.1%) for 5 min and blocked in BSA (5%) for 1 h. After blocking, cells were incubated with primary antibodies (anti-mTOR and anti-GNG7) at 4 °C overnight. PLA probes were then added, followed by hybridization, ligation, and amplification. Finally, cells were incubated with the detection solution and visualized by fluorescence microscopy.

Luciferase reporter assay

The human GNG7 promoter genomic region was amplified by PCR (Table S1) and then cloned into a pGL3-basic luciferase report vector. The mutant-binding sites were generated by site-directed mutagenesis (Table S1). The luciferase report vectors combined with the phRL-SV40 vector (an internal control) were transfected into 293T cells via polyetherimide, combined with either pLV-puro or pLV-FOXO3A. The luciferase activity was detected using the Dual Luciferase Report Gene Assay Kit (Beyotime) according to the manufacturer's instructions.

RNA-seq and cleavage under targets and tagmentation (CUT&Tag)

Total RNA samples were extracted from U-937 cells upon FOXO3A knockout. RNA-seq was performed by LianChuan Science (Hangzhou, China) and the libraries were sequenced by the Illumina HiSeq 2000 platform as 150-bp pair-ended reads. RNA-seq data were analyzed according to previous work.[21] The CUT&Tag assay and data processing were conducted as described previously.[21] Here, a total of 100,000 leukemia cells were harvested and the antibody against FOXO3A (#12829, Cell Signaling Technology) was used to detect the target DNA of FOXO3A.

Structure-based virtual screening of FOXO3A inhibitors

Briefly, the crystal structure of FOXO3A (PDB ID: 2UZK) was obtained from the RCSB protein data bank (http://www.rcsb.org/). Prior to virtual screening, a total of 2356 and 17,580 compounds from the L1000 and L6020 databases were filtered by pan-assay interference structures (PAINS).[22] Structure-based *in silico* screening of FOXO3A inhibitors was performed using Glide in Schrödinger software.[23] Residues in the crystal structure were defined as the binding site at which the docking grids were created. Two stages of virtual screening (SP: standard-precision mode; and XP: extra-precision mode) with increasing accuracy and computational cost was carried out. At each stage, only the top 10% scoring compounds were selected to advance to the next stage. FOXO3A ligand was docked and scored using the Glide SP mode and the best pose of the FOXO3A ligand was chosen using the Glide Score. The binding interaction model of the ligand with human FOXO3A was analyzed using Pymol. After the extra-precision screening, the structures and binding interaction modes of the retained compounds were analyzed and the final 5 compounds (TargetMol) were purchased for bioassay.

Statistics

All statistical analysis was performed using GraphPad Prism 8 software (GraphPad Software). Comparisons between groups were analyzed using a two-tailed Student's *t*-test or one-way ANOVA followed by Dunn's post hoc test. Survival analysis was performed using the Kaplan-Meier method with a log-rank (Mantel-Cox) comparison of survival curves. All data were expressed as mean ± standard deviation (SD). *P*-values <0.05 were considered statistically significant.

Results

FOXO3A deficiency induces myeloid maturation and apoptosis of AML cells

Highly *FOXO3A* expression has been revealed as an adverse prognostic factor in AML,[10,11] here we studied an AML patient cohort (TCGA) and found that elevated expression of *FOXO3A* correlated with overall shorter survival of AML patients (Fig. 1A). FOXOs have been found active in murine AML cells[9]; to determine the roles of FOXO3A in human AML cells, we further utilized the published single-cell RNA sequencing (RNA-seq) data based on 5 healthy donors and 16 AML patients.[24] We found that primitive AML cells (HSC-like, GMP-like, and ProMono-like malignant cells) showed

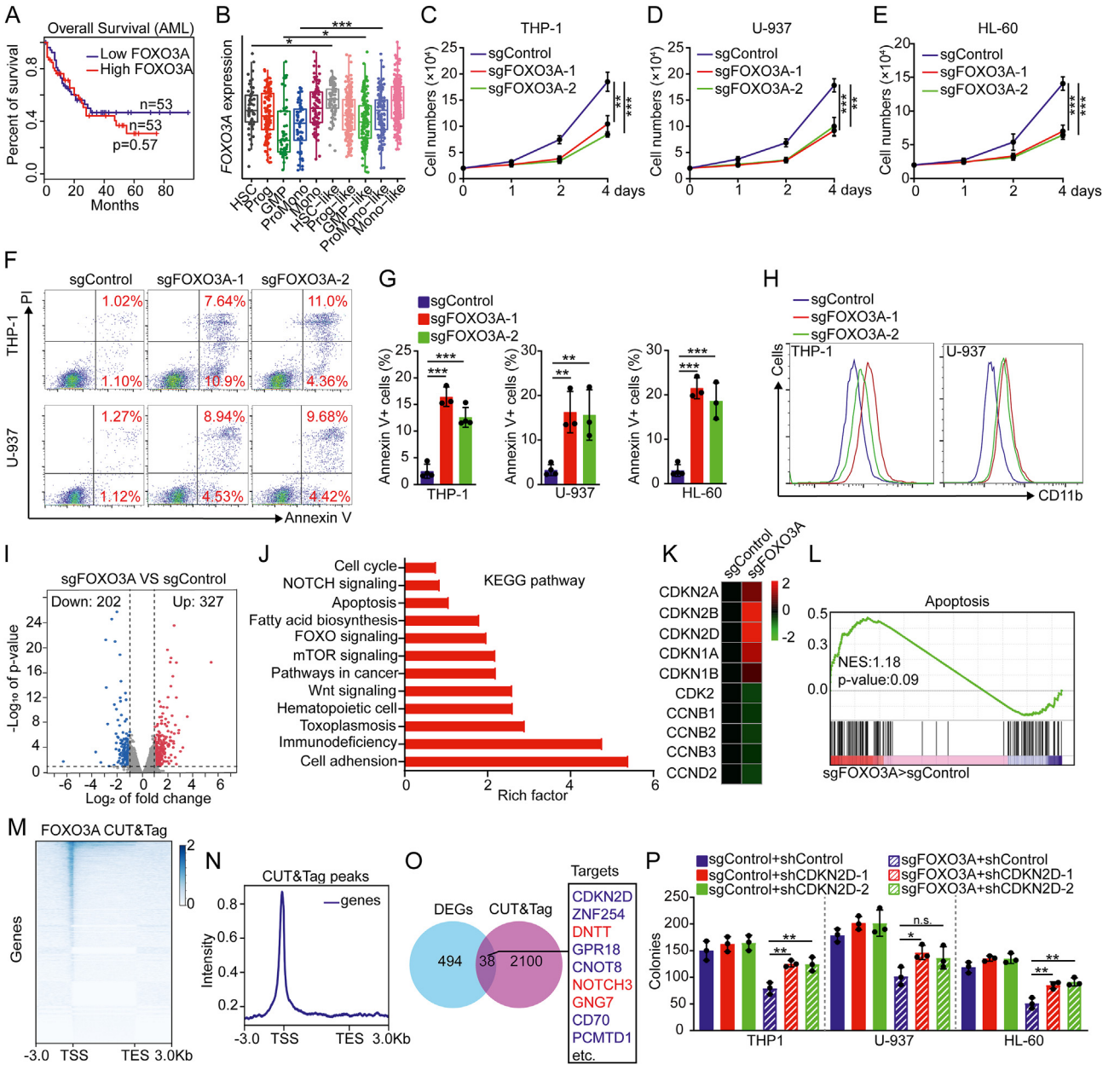

Figure 1 *FOXO3A* is essential for the maintenance of leukemia cells. **(A)** Kaplan-Meier plots of overall survival in the TCGA cohort for AML patients stratified based on *FOXO3A* expression above (FOXO3A^{high}) or below (FOXO3A^{low}) the median. **(B)** Single-cell RNA-seq data showing *FOXO3A* expression in healthy donor- and AML patient-derived BM cells. Each dot represents one cell. HSC, hematopoietic stem cell; Prog, progenitor; GMP, granulocyte-macrophage progenitor; Promono, promonocyte; Mono, monocyte. Data were from GSE116256. **(C–E)** Growth curves of leukemia cells after transduction with indicated lentivirus ($n = 4$). **(F, G)** Flow cytometry analysis of apoptosis in leukemia cells using Annexin V/PI staining. The histograms indicate the percentages of Annexin V$^+$ cells ($n = 3–4$). **(H)** Flow cytometry analysis of CD11b intensity in leukemia cells ($n = 3$). **(I)** Representative volcano of up-regulated genes or down-regulated genes by 2-fold or more in U-937 cells transduced with indicated lentivirus ($n = 3$). **(J)** KEGG pathway analysis of the differentially expressed genes in *FOXO3A*-deficient leukemia cells. **(K)** Heatmap of expression of indicated cell-cycle related genes ($n = 3$). Data were from RNA-seq. **(L)** GSEA plot showing enrichment of gene sets (apoptosis) in *FOXO3A*-deficient leukemia cells. Data were from RNA-seq. **(M)** Representative heatmap of genome-wide FOXO3A CUT&Tag signal around genes in U-937 cells. TSS, transcription start site; TES, transcription end site. **(N)** Average diagram of genome-wide FOXO3A CUT&Tag peaks at TSS and TES regions (±3000 bp). **(O)** Integrative analysis to identify transcriptome-wide potential targets of FOXO3A in leukemia cells. DEGs indicate genes with significantly increased or decreased expression upon *FOXO3A* depletion (FPKM >1, fold change >2). CUT&Tag indicates genes with significant enrichment in FOXO3A binding (reads per kilobase per million >1). Red indicates potential positive targets of FOXO3A and blue indicates potential negative targets of FOXO3A. **(P)** Colony-forming assay of control and *FOXO3A*-deficient leukemia cells with or without knockdown of *CDKN2D*. The number of colonies was counted at 6–7 days after plating 5000 leukemia cells ($n = 3$). Error bars represent mean ± SD. *$P < 0.05$, **$P < 0.01$, ***$P < 0.001$; n. s., no significance; one-way ANOVA.

higher expression of *FOXO3A* than their counterparts from the healthy donors (Fig. 1B). To determine the impact of *FOXO3A* deficiency on AML cells, we generated knockout (KO) cells of *FOXO3A* using two independent small guide RNAs (sgRNAs) (Fig. S1A). We found that *FOXO3A* depletion substantially inhibited the growth of AML cell lines with *MLL-AF9* translocations (THP-1 and HL-60), as well as an AML cell line that does not carry *MLL* translocations (U-937) (Fig. 1C—E). Annexin V and PI staining showed that *FOXO3A* deficiency induced the apoptosis of AML cells (Fig. 1F, G). Moreover, the expression of the myeloid maturation marker (CD11b) was higher on *FOXO3A*-deficient cells (Fig. 1H), suggesting that FOXO3A inhibited myeloid differentiation.

FOXO3A sustains the proliferation of AML cells partially via CDKN2D

As a transcription factor, FOXO3A regulating gene expression shows cell-type dependence[7] and the exact targets of FOXO3A in AML cells remain unclear. To explore the underlying molecular mechanisms of FOXO3A-regulated AML cell function, we performed RNA-seq analysis and found that 327 genes in *FOXO3A*-deficient U-937 cells were considerably up-regulated compared with control cells, while 202 genes were significantly down-regulated (>2-fold change; $P < 0.01$; Fig. 1I). The major signaling pathways enriched with the differentially expressed genes including hematopoietic cell lineage, Wnt signaling, mTOR signaling, FOXO signaling, apoptosis, NOTCH signaling, and cell cycle (Fig. 1J). Specifically, several genes encoding cyclin-dependent kinase inhibitors showed elevated expression, including *CDKN2A*, *CDKN2B*, and *CDKN2D*. In contrast, multiple genes encoding cyclins or cyclin-dependent kinases showed decreased expression, including *CCNB1*, *CCNB2*, *CCNB3*, and *CDK2* (Fig. 1K), suggesting that *FOXO3A* deficiency inhibited cell cycling of AML cells at the molecular level. Gene set enrichment analysis (GSEA) of the RNA-seq data further revealed that the set of genes up-regulated in *FOXO3A*-deficient cells showed enrichment for apoptosis and cytokine receptor interaction, while the set of genes down-regulated showed enrichment for NOTCH signaling and Wnt beta-catenin signaling (Fig. 1L; Fig. S1B—D).

To search the direct targets of FOXO3A, we profiled the genome-wide FOXO3A binding site utilizing FOXO3A cleavage under targets and tagmentation (CUT&Tag) strategy with U-937 cells. The CUT&Tag data based on *FOXO3A*-deficient cells showed no obvious peaks (Fig. S1E, F), while the data based on control cells showed that FOXO3A mainly bound to transcription start site (TSS) regions of the genes (Fig. 1M, N), confirming the specially and transcriptionally regulatory roles of FOXO3A in AML cells. Through integrative analysis of RNA-seq and CUT&Tag data, we identified 38 genes directly regulated by FOXO3A, including genes up-regulated by FOXO3A (*e.g.*, *DNTT*, *NOTCH3*, and *GNG7*) and genes down-regulated by FOXO3A (*e.g.*, *CDKN2D*, *ZNF254*, and *GPR18*) (Fig. 1O and Table S2). To substantiate these data, we conducted a chromatin immunoprecipitation PCR assay (ChIP-PCR) and demonstrated the occupancy of FOXO3A at promoter regions of *NOTCH3*, *CDKN2D*, *CD70*, and *DNTT* (Fig. S1G). Moreover, the quantitative RT-PCR (qRT-PCR) data verified the change in gene expression observed in RNA-seq data (Fig. S1H). Consistently, we found evident binding peaks of FOXO3A at TSS or TES of these targets, associated with the changed abundance of RNA-seq peaks (Fig. S1I). *NOTCH3* has been demonstrated to promote AML transformation and progression,[25] while *CDKN2D* is a well-known growth repressor in leukemia.[26] To determine whether FOXO3A preserved AML cell expansion by inhibiting the expression of *CDKN2D*, we knocked down the expression of *CDKN2D* using two independent short hairpin RNAs (shRNAs). We observed that the knockdown of *CDKN2D* partially restored the colony-forming capacity of *FOXO3A*-deficient cells (Fig. 1P), suggesting that FOXO3A sustained AML cell expansion partially via inhibiting the expression of *CDKN2D*.

mTOR activity is elevated in AML cells with *FOXO3A* depletion

It has been revealed that *FOXO3A* deficiency inversely activates JNK/c-JUN signaling that weakens the cytotoxic effect of *FOXO3A* depletion on AML cells,[9] suggesting the phenomenon of adaptive resistance of AML cells to FOXO3A inhibition. Here, we found that the set of up-regulated genes showed enrichment for up-regulated gene set encoding products correlated with PI3K- Akt and mTORC1 (mTOR complex 1) pathways (Fig. 1I, 2A). It has been revealed that mTOR is hyperactivated in approximately 60% of AML patients and mTOR is essential for the proliferation and survival of leukemia cells.[27,28] To further explore the response of mTOR signaling to FOXO3A inhibition, we used phospho-flow analysis and observed an elevated level of phospho-mTOR (p-mTOR) in *FOXO3A*-deficient cells compared with their counterparts, as well as for the p-S6 intensity in *FOXO3A*-deficient cells, a well-known downstream protein of mTOR by phosphorylation (Fig. 2B—D). Moreover, the Western blot results confirmed that *FOXO3A* deficiency elevated the level of p-mTOR and p-S6 (Fig. 2E). Consistent with previous findings,[9] we also found that loss of *FOXO3A* resulted in substantially increased protein levels of p-JNK, p-C-JUN, and total C-Jun (Fig. 2E). The mTOR signaling governs cell mitochondrial metabolism that produces energy for cells and affects multiple signaling, eventually playing a vital role in the growth and maturation of leukemia cells.[27] To acquire further insight into the mitochondrial metabolism of AML cells after *FOXO3A* deletion, we analyzed the mitochondrial count in AML cell lines using mitochondrial DNA measurement. We observed increased mitochondrial mass in *FOXO3A*-deficient cells compared with control cells, as well as increased ATP production (Fig. S2A, B). To further strengthen the above results, we utilized DCFH-DA to detect ROS produced by mitochondrial metabolism and observed elevated ROS levels in *FOXO3A*-deficient cells (Fig. S2C), suggesting that *FOXO3A* deficiency elevated mitochondrial metabolism.

To determine whether the increased mTOR activity contributed to the increased mitochondrial metabolism, we administrated rapamycin treatment to inhibit mTOR activity. Notably, the increased mitochondrial mass and ATP production in *FOXO3A*-deficient cells were considerably abolished by rapamycin treatment (Fig. S2D, E). The JNK/C-JUN signaling is critical for the survival of AML cells,[9,29] and

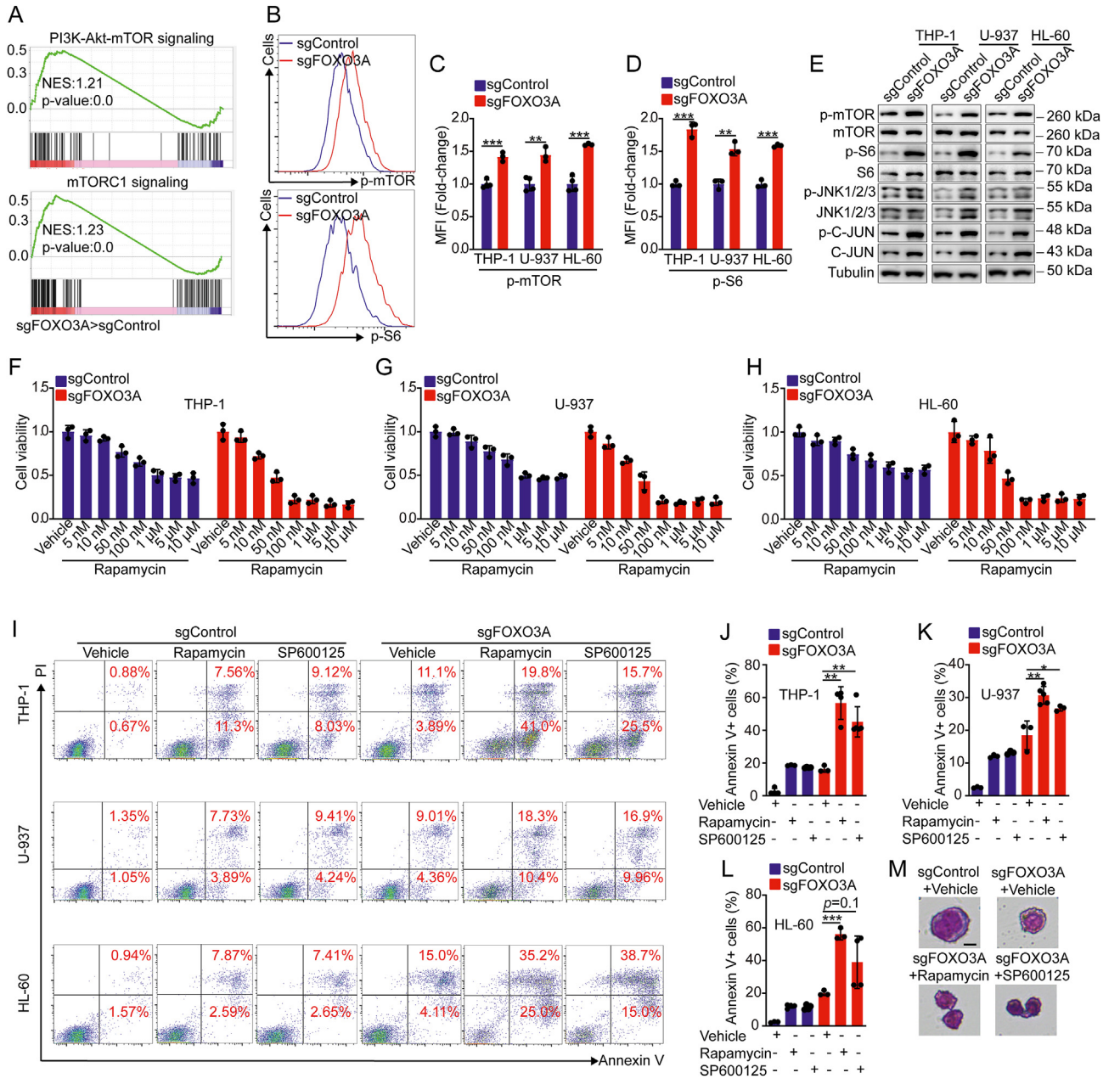

Figure 2 *FOXO3A* deficiency activates mTOR signaling. **(A)** GSEA plot showing enrichment of gene sets in *FOXO3A*-deficient leukemia cells. Data were from RNA-seq. **(B—D)** Flow cytometry analysis of p-mTOR and p-S6 in leukemia cells transduced with the indicated lentivirus. The histograms indicate the mean fluorescence intensity (MFI) analysis of p-mTOR and p-S6 ($n = 3$—4). **(E)** Western blot of indicated proteins in lysates prepared from leukemia cells ($n = 3$). **(F—H)** *In vitro* cell viability assay of leukemia cells using CCK8, with the treatment of different doses of rapamycin for 48 h ($n = 3$). **(I—L)** Flow cytometry analysis of apoptosis in leukemia cells using Annexin V/PI staining, with the treatment of rapamycin (100 nM) or SP600125 (5 μM) for 48 h. The histograms indicate the percentages of Annexin V^+ cells ($n = 3$—5). **(M)** Representative images of Wright-Giemsa staining of U-937 cells with indicated drug treatment. Scale bar = 10 μm. Error bars represent mean ± SD. $^*P < 0.05$, $^{**}P < 0.01$, $^{***}P < 0.001$; n. s., no significance; one-way ANOVA.

it has been demonstrated that ROS generated by mitochondrial metabolism induces activation of JNK/C-JUN signaling.[30,31] Thus, we speculated that FOXO3A inhibition induced activation of JNK/C-JUN via mTOR signaling. To confirm the hypothesis, we treated *FOXO3A*-deficient cells with rapamycin or a ROS scavenger N-acetyl-cysteine (NAC). We observed an efficient decreased ROS level and decreased protein levels of p-JNK and p-C-JUN in *FOXO3A*-deficient cells with the addition of rapamycin or NAC (Fig. S2F, G), indicating that *FOXO3A* depletion induced inverse activation of JNK/C-JUN via the mTOR-ROS axis.

To test whether the elevated mTOR and JNK/C-JUN activity antagonized the growth inhibition and apoptosis mediated by *FOXO3A* depletion in AML cells, we treated

AML cells with a series of doses of mTOR inhibitor (rapamycin) or JNK inhibitor (SP600125). With the treatment of rapamycin or SP600125, *FOXO3A*-deficient cells showed more obvious growth arrestment compared with sgControl cells (Fig. 2F—H; Fig. S3A, B), suggesting that inhibition of mTOR or JNK enhanced the cytotoxic effect of *FOXO3A* depletion on AML cells. To further explore the combinatorial effects, we performed a colony-forming assay and found that *FOXO3A*-deficient cells with the treatment of rapamycin gave rise to a minimum number of total colonies (Fig. S3C—E). Moreover, the Annexin V and PI staining showed that the addition of rapamycin or SP600125 both induced significantly increased apoptosis in *FOXO3A*-deficient cells compared with *FOXO3A* depletion alone, and rapamycin treatment was superior to SP600125 addition (Fig. 2I—L). To further strengthen these data, we performed Wright-Giemsa staining and found that the addition of rapamycin or SP600125 to *FOXO3A*-deficient U-937 cells resulted in morphological change consistent with myeloid maturation and apoptosis (Fig. 2M). Together, these results revealed that FOXO3A inhibition induced reactive activation of mTOR signaling, and combinatorial inhibition of FOXO3A and mTOR was an effective approach to kill AML cells.

Combinatorial inhibition of mTOR and FOXO3A displays anti-AML efficacy *in vivo*

To further test the potential of combinatorial inhibition of FOXO3A and mTOR in AML therapy, immunodeficient mice (NOD/SCID) transplanted with U-937 AML cells were treated with either rapamycin (4 mg/kg, i.p., three times a week)[32] or SP600125 (15 mg/kg, i.p., three times a week),[33] or vehicle for three weeks (Fig. 3A). Human CD45 (hCD45) detection showed that *FOXO3A* deficiency

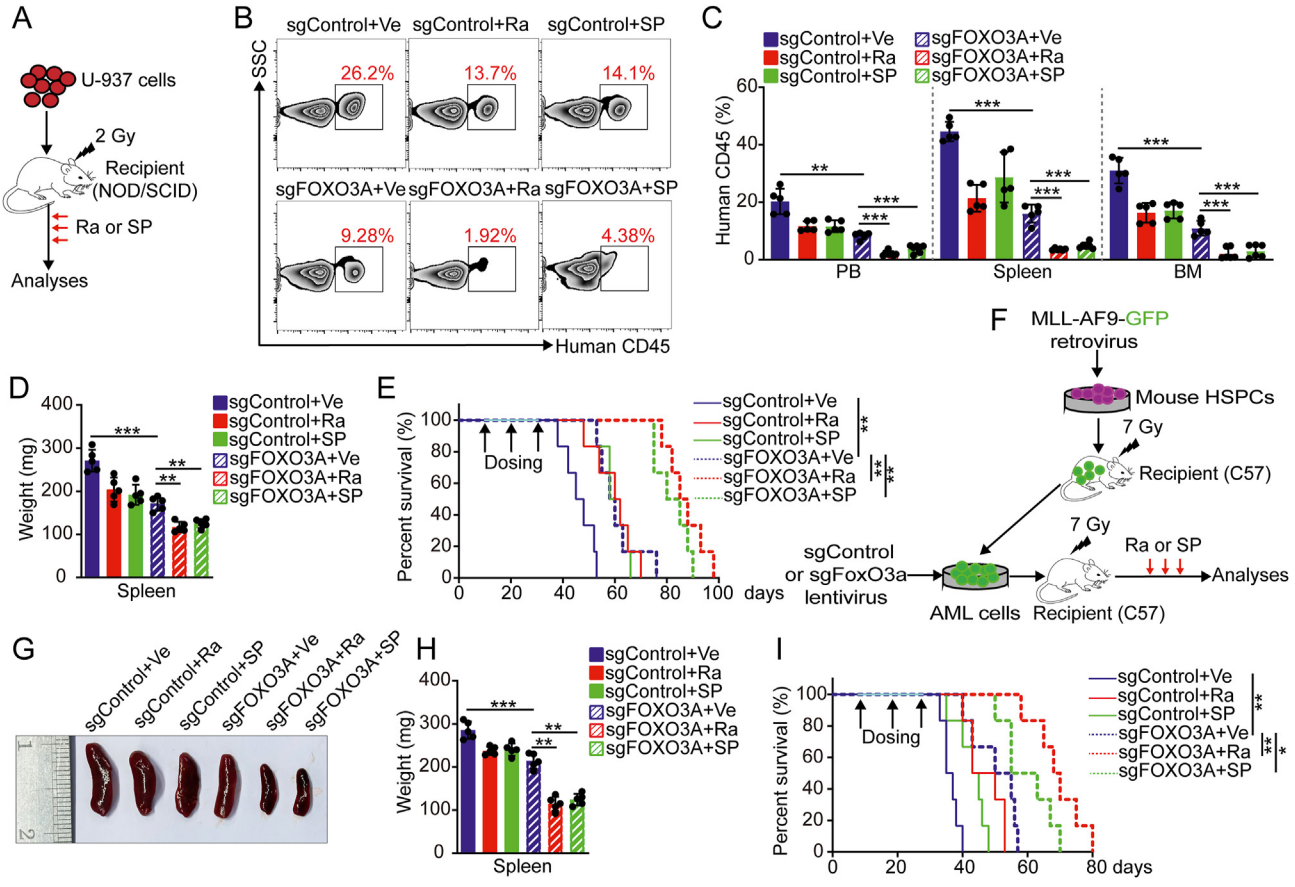

Figure 3 Combinatorial inhibition of mTOR and FOXO3A suppresses AML *in vivo*. **(A)** Experimental schematic for AML cell line-derived xenograft. After 10 days of transplantation, NOD/SCID mice were treated with vehicle (Ve), rapamycin (Ra) (4 mg/kg, i. p. injection; three times a week), SP600125 (SP) (15 mg/kg, i. p. injection; three times a week), or a combination (rapamycin plus SP600125) for three weeks. **(B, C)** Flow cytometry analysis of human-CD45-positive leukemia cells in PB, spleen, and BM of recipient mice at the end of treatment. The histograms indicate the percentages of $hCD45^+$ leukemia cells in PB ($n = 5$—7). **(D)** Spleen weight analysis of recipient mice at the end of treatment ($n = 5$). **(E)** Kaplan-Meier survival of the mouse cohorts ($n = 6$ each) with indicated treatment. **(F)** Experimental schematic for murine *MLL-AF9* leukemia model. After the second transplantation, recipient mice were treated with the vehicle, rapamycin (4 mg/kg, i. p. injection; three times a week), SP600125 (15 mg/kg, i. p. injection; three times a week), or a combination (rapamycin plus SP600125) for three weeks. **(G)** Spleen image of recipient mice at the end of inhibitor treatment. **(H)** Spleen weight analysis of recipient mice at the end of treatment ($n = 5$). **(I)** Kaplan—Meier survival of the mouse cohorts ($n = 6$ each) with indicated treatment. Error bars represent mean ± SD. $^*P < 0.05$, $^{**}P < 0.01$, $^{***}P < 0.001$; one-way ANOVA or Mantel-Cox test.

attenuated engraftment of leukemia cells in peripheral blood (PB) of mice, and the treatment of rapamycin or SP600125 both resulted in a substantial reduction in leukemia burden of mice (transplanted *FOXO3A*-deficient cells) compared with their counterparts (Fig. 3B, C). Moreover, the treatment of rapamycin resulted in the least splenomegaly in mice (transplanted *FOXO3A*-deficient cells) (Fig. 3D), as well as minimum $hCD45^+$ infiltrates in the spleen and bone marrow (BM) (Fig. 3C). Consistent with the antileukemic activity of combinatorial inhibition of FOXO3A and mTOR, mice that received rapamycin treatment showed statistically longest survival (Fig. 3E), validating the combinatorial approach for treating AML by dual inhibition of FOXO3A and mTOR. To test whether combinatorial inhibition of mTOR and FOXO3A suppressed murine leukemogenesis, hematopoietic stem/progenitor cells (HSPCs) from wild-type C57BL/6 J mice were transduced with *MLL-AF9-GFP* retrovirus to generate AML mice. Next, the sorted leukemia cells (GFP^+ BM cells) from AML mice were transduced with sgFoxO3a lentivirus to deplete *FoxO3a* and then transplanted into lethally irradiated recipient mice (Fig. 3F). Consistently, dual inhibition of FoxO3a and mTOR resulted in relieved splenomegaly, along with decreased spleen weight (Fig. 3G, H). Moreover, this combinatory approach substantially diminished the percentage of leukemia cells (GFP^+) in PB, spleen, and BM in recipient mice (Fig. S3F). Recipient mice of *MLL-AF9*-transduced *FoxO3a*-deficient HSPCs developed and died of AML significantly slower than recipients of *MLL-AF9*-transduced wild-type HSPCs (Fig. 3I), while rapamycin or SP600125 treatment further prolonged the survival of AML recipients (Fig. 3I). Thus, these data demonstrated that combinatory inhibition of FOXO3A and mTOR efficiently delayed AML progression *in vivo*.

FOXO3A inversely inhibits mTOR via its transcriptional target GNG7

To further explore the underlying molecular mechanisms of FOXO3A regulating mTOR activity, we analyzed the expression of mTOR upon *FOXO3A* depletion in AML cells. The mRNA and protein levels of mTOR were comparable in sgControl and sgFOXO3A cells (Fig. S4A; Fig. 2E), suggesting that FOXO3A regulated the phosphorylation of mTOR, rather than the expression of total mTOR. It has been revealed that the regulators of mTOR, tuberous sclerosis complex proteins 1 (*TSC1*), *Sestrin3*, and *Rictor* are transcriptional targets of FOXOs[34,35]; however, the expression of the above-mentioned genes in *FOXO3A*-deficient cells showed no obvious change (Fig. S4B). Next, we screened the mediator of FOXO3A regulating mTOR activity via integrative analysis of differentiated genes (data from RNA-seq) and the upstream regulators of mTOR (*e.g.*, small GTPases, kinases, G-protein-coupled receptors, growth factors)[36] (Fig. 4A). Importantly, we identified a novel modulator, the *G* protein gamma subunit 7 (GNG7) (Fig. 1O, 4A), which is a subunit of heterotrimeric *G* protein and ubiquitously expressed in multiple cells but is down-regulated in various cancers.[37,38] *G* proteins interact with multiple effector molecules such as phospholipase and *G* protein-coupled receptor kinases (GRK) for downstream signal transduction.[39,40] It has been revealed that GNG7 is associated with mTOR activity, but the underlying mechanisms remain largely unknown.[41–43] Here, we found an interaction between GNG7 and mTOR via the immunoprecipitation assay (Fig. 4B). We further confirmed a physical interaction between GNG7 and mTOR via the *in situ* proximity ligation assay (PLA) (Fig. 4C), implying that GNG7 affected mTOR activation via direct interaction. Indeed, we knocked out *GNG7* in AML cells via sgRNA and found that loss of *GNG7* substantially elevated the p-mTOR level, as well as p-C-JUN and total C-JUN levels (Fig. 4D). The phosphor-flow analysis showed an elevated level of p-mTOR in *GNG7*-deficient cells compared with their counterparts (Fig. 4E), demonstrating that GNG7 inhibited phosphorylated activation of mTOR.

Further, we found that loss of *FOXO3A* decreased the expression of *GNG7* mRNA and protein (Fig. 4F, G), implying that GNG7 was a potential mediator of FOXO3A regulating mTOR activity. To determine whether *GNG7* was a direct transcriptional target of FOXO3A, we analyzed the CUT&Tag data and found obvious FOXO3A-CUT&Tag peaks at the promoter regions of GNG7 (Fig. 4H), implying a regulatory effect of FOXO3A on *GNG7* transcription. Next, we searched for the consensus FOXO3A-binding site (GTAAACAA) in the proximal promoter regions of *GNG7* and found four potential binding sites (Fig. 4I). The ChIP assay revealed the direct binding of FOXO3A to site 3 at promoter regions of *GNG7* (Fig. 4J). The luciferase activity of a construct containing the wild-type-binding site showed apparent increases in *FOXO3A* expression, but the construct with a mutant binding site did not (Fig. 4K, L), indicating that FOXO3A directly bound to the promoter regions and induced expression of *GNG7*. To further determine whether the decreased GNG7 level contributed to the reactive activation of mTOR in *FOXO3A*-deficient cells, we administered lentivirus transduction to induce *GNG7* overexpression in *FOXO3A*-deficient cells. *GNG7* overexpression efficiently restricted activation of mTOR and C-JUN induced by *FOXO3A* depletion (Fig. 4M), suggesting a FOXO3A-GNG7-mTOR regulatory axis. Moreover, restoring the expression of *GNG7* in *FOXO3A*-deficient cells enhanced the inhibitory effect of *FOXO3A* depletion on the colony-forming capacity of AML cells (Fig. 4N). Taken together, these data suggested that FOXO3A inversely inhibited mTOR via its transcriptional target GNG7.

Structure-based virtual screening and validation assays identify Gardenoside as a potential FOXO3A inhibitor

To identify potential FOXO3A inhibitors, we conducted a FOXO3A DNA-binding domain (DBD) structure-based virtual screening of the compounds from the Approved Drug Library (L1000) and the Selected Natural Compound Library (L6020) (Fig. 5A, B). The three-dimensional structure of FOXO3A DBD was obtained from RCSB Protein Data Bank (PDB id 2UZK).[44,45] The helix 3 subunit of FOXO3A DBD is essential for DNA recognition and binding.[45] We obtained the top 5 candidate compounds that showed the highest scores based on their docking to FOXO3A's helix 3 pockets (Fig. 5B, C). The docking models suggested that the five

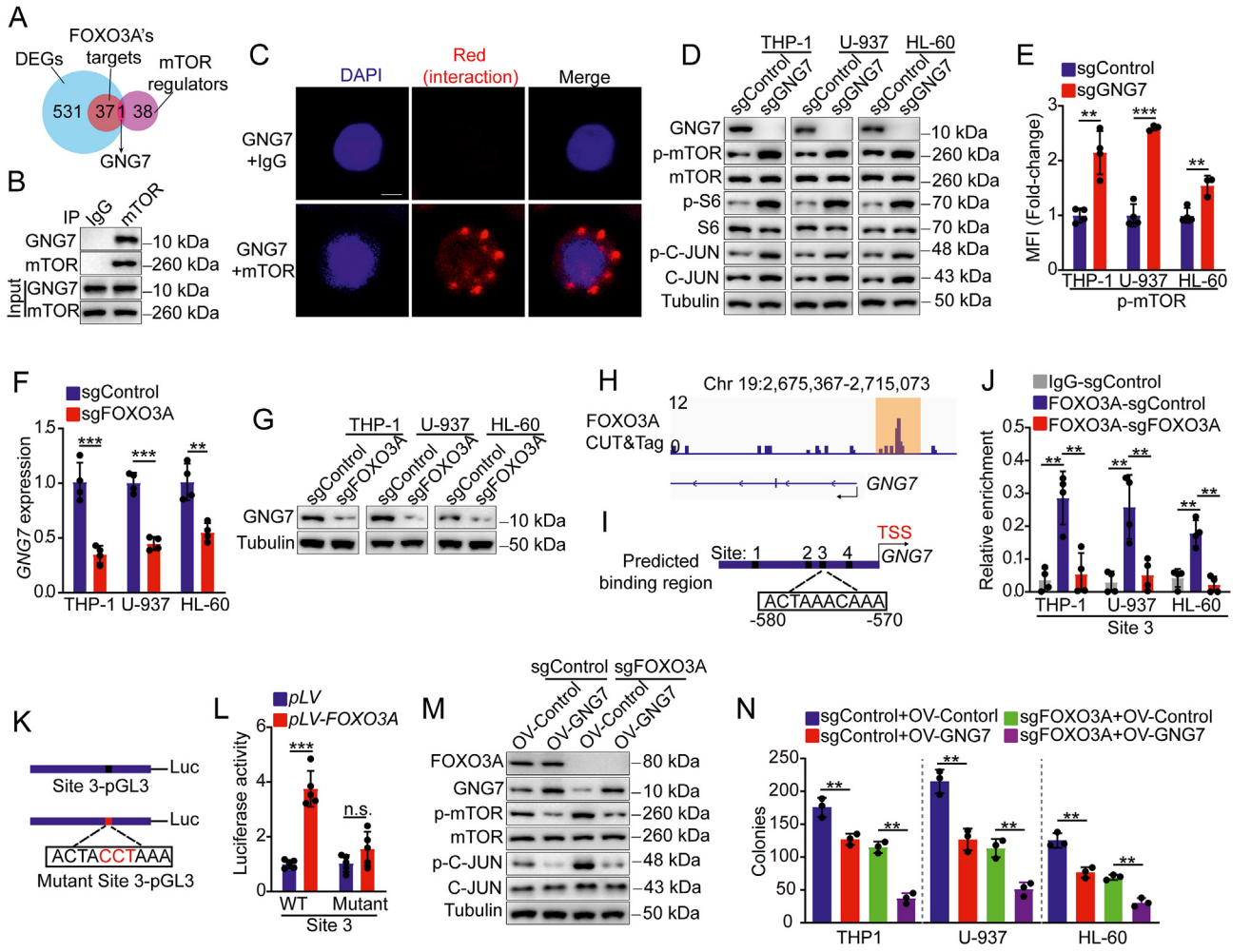

Figure 4 FOXO3A inversely inhibits mTOR via its transcriptional target GNG7. **(A)** Integrative analysis to identify targets of FOXO3A regulating mTOR activity in leukemia cells. DEGs indicate genes with significantly increased or decreased expression upon *FOXO3A* depletion. mTOR regulators indicated genes reported to function as upstream regulators of mTOR. **(B)** Western blot of proteins immunoprecipitated from cell lysates of U-937 cells ($n = 3$). WCL, whole-cell lysates. **(C)** *In situ* ligation assay to detect GNG7/mTOR interaction in U-937 cells. As a negative control, proximity ligation was performed using an anti-GNG7 antibody and IgG. Nuclei were visualized using DAPI staining. Scale bar = 10 μm. **(D)** Western blot of indicated proteins in lysates prepared from leukemia cells transduced with indicated lentivirus ($n = 3$) **(E)** Flow cytometry analysis of p-mTOR in leukemia cells. The histograms indicate the MFI analysis of p-mTOR ($n = 3$–4). **(F)** Relative mRNA expression of *GNG7* in leukemia cells ($n = 4$). **(G)** Western blot of GNG7 protein in lysates prepared from leukemia cells ($n = 3$). **(H)** FOXO3A CUT&Tag peaks around the *GNG7* gene loci. **(I)** The predicated FOXO3A-binding sites (black) in the upstream promoter regions of the human *GNG7* gene. **(J)** Quantitative ChIP-PCR was utilized to detect the binding of FOXO3A at the promoter regions of *GNG7* in leukemia cells ($n = 4$). IgG served as a negative control. Enrichment relative to the input is shown. **(K)** Schematic for wild-type and mutant *GNG7* promoter-luciferase constructs. **(L)** Luciferase activity analysis in 293T cells transfected with a luciferase-reported vector (PGL3) with the wild-type or mutant promoter of GNG7, as well as pLV and pLV-FOXO3A constructs ($n = 5$). **(M)** Western blot of indicated proteins in lysates prepared from control and *FOXO3A*-deficient cells (THP-1) with or without overexpression (OV) of *GNG7* ($n = 3$). **(N)** Colony-forming assay of control and *FOXO3A*-deficient leukemia cells with or without overexpression of *GNG7*, the number of colonies was counted at 6–7 days after plating 5000 leukemia cells ($n = 3$). Error bars represent mean ± SD. $^{*}P < 0.05$, $^{**}P < 0.01$, $^{***}P < 0.001$; n. s., no significance; Student's *t*-test or one-way ANOVA.

inhibitors bound tightly to FOXO3A protein and blocked its helix 3 pockets (Fig. 5D). We then assessed the effect of these compounds on FOXO3A inhibition and identified three compounds (STOCK1N-05715, STOCK1N-50932, and Gardenoside) that displayed significant effects on the expression of FOXO3A's target (*GNG7* or *CDKN2D*) (Fig. 5E). Through the luciferase reported assay, we discovered that Gardenoside inhibited FOXO3A binding DNA with a half-maximal inhibitory concentration (IC50) of 7.1 μM, which was superior to STOCK1N-05715 and STOCK1N-50932 (Fig. 5F). Gardenoside is a natural compound extracted from the fruits of Gardenia and shows hepatoprotective potential.[46] We found that Gardenoside interacted with the helix 3 subunits by forming hydrogen bonds with DCB10,

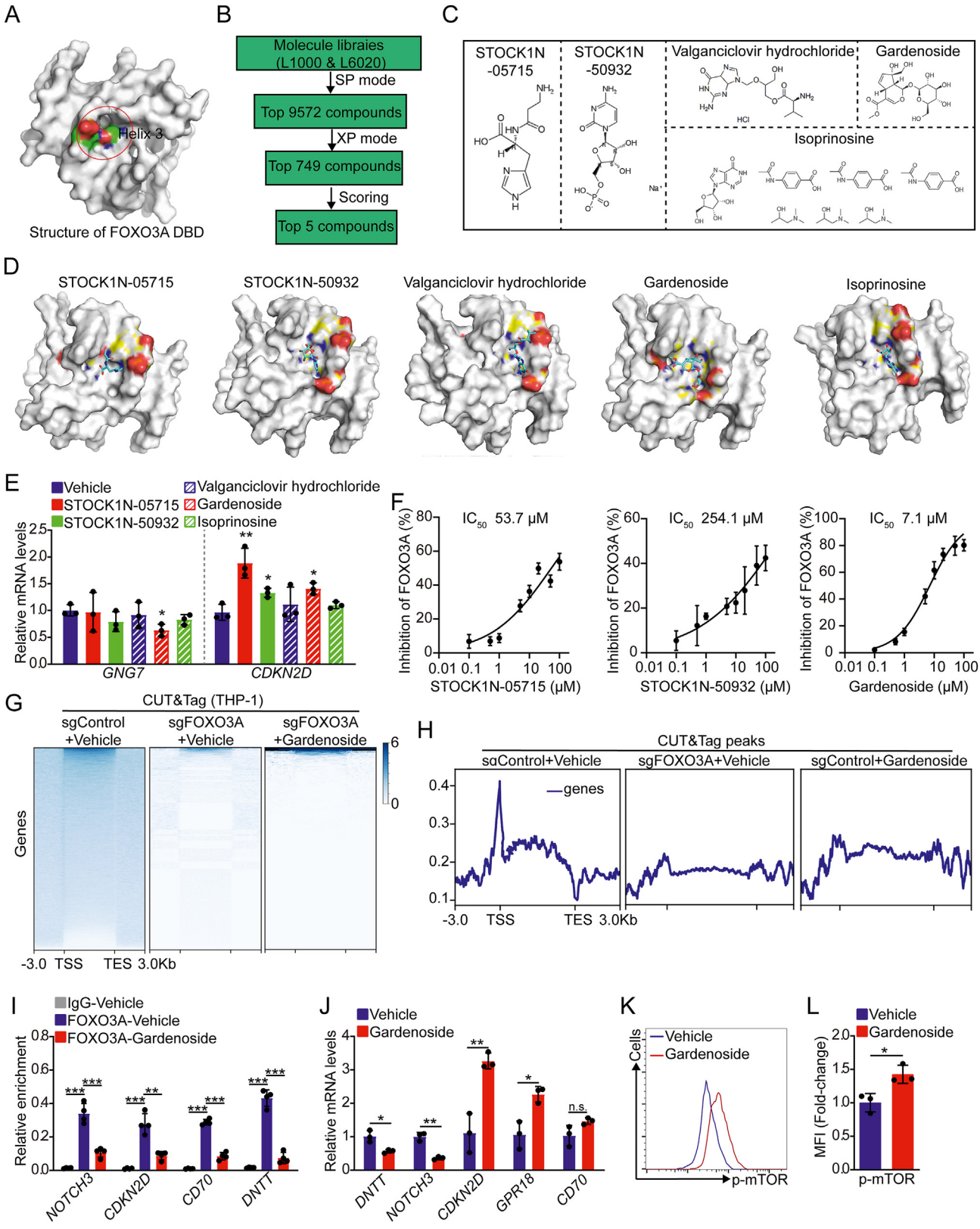

Figure 5 Identification of FOXO3A inhibitors through structure-based virtual screening. **(A)** Pyramid flowchart to identify FOXO3A from the Approved Drug Library (L1000) and the Selected Natural Compound Library (L6020). **(B)** Docking models were developed based on the crystal structure of the FOXO3A DNA-binding domain (DBD). The red round indicates helix 3 pockets. **(C)** The two-dimensional structure of the top 5 candidate compounds. **(D)** Binding model of top 5 candidate compounds in FOXO3A helix 3 pockets. **(E)** Relative mRNA expression of *GNG7* and *CDKN2D* in U-937 cells with the treatment of the vehicle or indicated molecules (5 μM) for 24 h. **(F)** Inhibition of 3 candidate compounds on FOXO3A DNA binding *in vitro* using luciferase activity analysis. 293T cells

DAB9, DCA8, Lys207, and Asn208 (Fig. S4C). To further confirm the inhibitory effect of Gardenoside on FOXO3A DNA binding, we conduct CUT&Tag analysis and found that *FOXO3A* depletion and Gardenoside treatment both led to rare FOXO3A-binding peaks (Fig. 5G, H), while Gardenoside treatment had no considerable effect on the abundance of FOXO3A protein (Fig. S4D). Moreover, the ChIP-PCR assay revealed that the Gardenoside treatment substantially impeded FOXO3A binding to the promoter regions of its targets (*NOTCH3*, *CDKN2D*, *CD70*, and *DNTT*) (Fig. 5I; Fig. S1G). Consistently, Gardenoside treatment induced the altered expression of genes in AML cells, like the change in *FOXO3A*-deficient cells (Fig. 5J; Fig. S1H). Moreover, Gardenoside treatment also resulted in the decreased expression of *GNG7* and subsequently induced reactive activation of mTOR in AML cells (Fig. 5E, K, L). Altogether, our data revealed that Gardenoside was a potential inhibitor of FOXO3A, and Gardenoside treatment could impair the transcriptionally regulatory function of FOX3A. Nevertheless, whether Gardenoside affected other targets requires further exploration.

Gardenoside combined with rapamycin delays AML progression *in vivo*

To assess the therapeutic potential of Gardenoside in AML, we treated AML cells with a series of doses of Gardenoside, we found that Gardenoside treatment inhibited the expansion of AML cells (Fig. 6A–C). With the treatment of rapamycin, Gardenoside-treated cells showed more obvious growth arrest compared with their counterparts (Fig. 6A–C), suggesting that inhibition of mTOR enhanced the cytotoxic effect of Gardenoside. To further explore the combinatorial effects, we performed a colony-forming assay and found that the combinatorial treatment of Gardenoside and rapamycin gave rise to a minimum number of total colonies of AML cells (Fig. 6D). Moreover, the Annexin V and PI staining showed that the dual addition of Gardenoside and rapamycin resulted in significantly increased apoptosis in AML cells compared with single-agent treatment (Fig. S4E–G), suggesting the combinatorial toxicity. To further assess the therapeutic potential of Gardenoside in inhibiting human primary AML cells, leukemia cells from three AML patients were treated with Gardenoside and rapamycin. Gardenoside and rapamycin both suppressed the proliferation of all three sets of primary AML cells (Fig. 6E). Notably, the combinatorial of Gardenoside and rapamycin led to a severely decreased cell growth compared with single-agent treatment (Fig. 6E). Moreover, Gardenoside combined with rapamycin resulted in markedly reduced sizes of colonies from patient leukemia cells (Fig. 6F), suggesting that the leukemia malignancy of combinatorial-treated AML cells was substantially impaired.

To evaluate the therapeutic efficacy of the combinatorial approach *in vivo*, we transplanted primary AML cells into sub-lethally irradiated NOD/SCID mice, generating a patient-derived xeno-transplantation (PDX) AML mouse model. The recipient mice were treated with Gardenoside (15 mg/kg, i. p, three times/week) or rapamycin (4 mg/kg, i. p, three times/week), or vehicle for three weeks (Fig. 6G). Flow cytometry analysis of engrafted AML cells in recipient mice by hCD45 staining revealed a considerably decreased proportion of AML blast in PB upon Gardenoside or rapamycin treatment, and the combination treatment showed the best efficiency (Fig. 6H, I). Recipient mice treated with Gardenoside or rapamycin had a longer median survival (66.5 and 63 days, respectively); overall, mice receiving combination treatment had a statistically longer survival (88 days) (Fig. 6J). To determine the safety of the combinatory approach for *in vivo* treatment, we examined the toxic effects of the combinatorial use of Gardenoside and rapamycin on C57BL/6 J mice over 4 weeks (Fig. 6K). We observed no evidence of body weight loss (Fig. 6L) nor any physical damage on multiple organs (Fig. 6M). We found that the total number of BM cells, hematopoietic progenitor cells (HPC), and $Lin^{-}Sca\text{-}1^{+}c\text{-}Kit^{+}$ (LSK) cells showed negligible change with or without inhibitor treatment (Fig. 6N–P). The frequency and the total number of hematopoietic stem cells (HSC) ($CD34^{-}LSK$) also exhibited slight change, but the total number of long-term HSC ($CD48^{-}CD150^{+}LSK$, named SLAM HSC) was decreased in the inhibitor-treated mice compared with their counterparts (Fig. 6Q, R). Taken together, our data indicated that Gardenoside combined with rapamycin partially repressed hematopoiesis, but efficiently delayed AML progression and improved survival *in vivo*.

Discussion

It has been revealed that FOXO3A has crucial roles in hematopoiesis and leukemogenesis, and loss of *FOXO3A* induces apoptosis and myeloid maturation of AML cells.[8,9] Here, we further uncovered the underlying molecular mechanisms of FOXO3A preserving AML cells, as well as the unrecognized molecular reactivation to FOXO3A inhibition. We discovered that FOXO3A restricted the activation of mTOR signaling by transcriptionally inducing the expression of *GNG7*, which directly interacted with mTOR and inhibited the activation of its phosphorylation. Based on these

were transfected with a luciferase-reported vector (PGL3) with the wild-type promoter of *GNG7* and pLV-FOXO3A constructs. **(G)** Representative heatmap of genome-wide FOXO3A CUT&Tag signal around genes in control and *FOXO3A*-deficient cells (THP-1) with or without treatment of Gardenoside (5 μM). TSS, transcription start site; TES, transcription end site. **(H)** Average diagram of genome-wide FOXO3A CUT&Tag peaks at TSS and TES regions (±3000 bp). **(I)** Quantitative ChIP-PCR was utilized to detect the binding of FOXO3A at the promoter regions of indicated genes in U-937 cells ($n = 4$). IgG served as a negative control. Enrichment relative to the input is shown. **(J)** Relative mRNA expression of indicated genes in U-937 cells with the treatment of vehicle or Gardenoside (5 μM) for 48 h ($n = 3$). **(K, L)** Flow cytometry analysis of p-mTOR in U-937 cells. The histograms indicate the MFI analysis of p-mTOR ($n = 3–4$). Error bars represent mean ± SD. $^{*}P < 0.05$, $^{**}P < 0.01$, $^{***}P < 0.001$; n. s., no significance; Student's *t* test or one-way ANOVA.

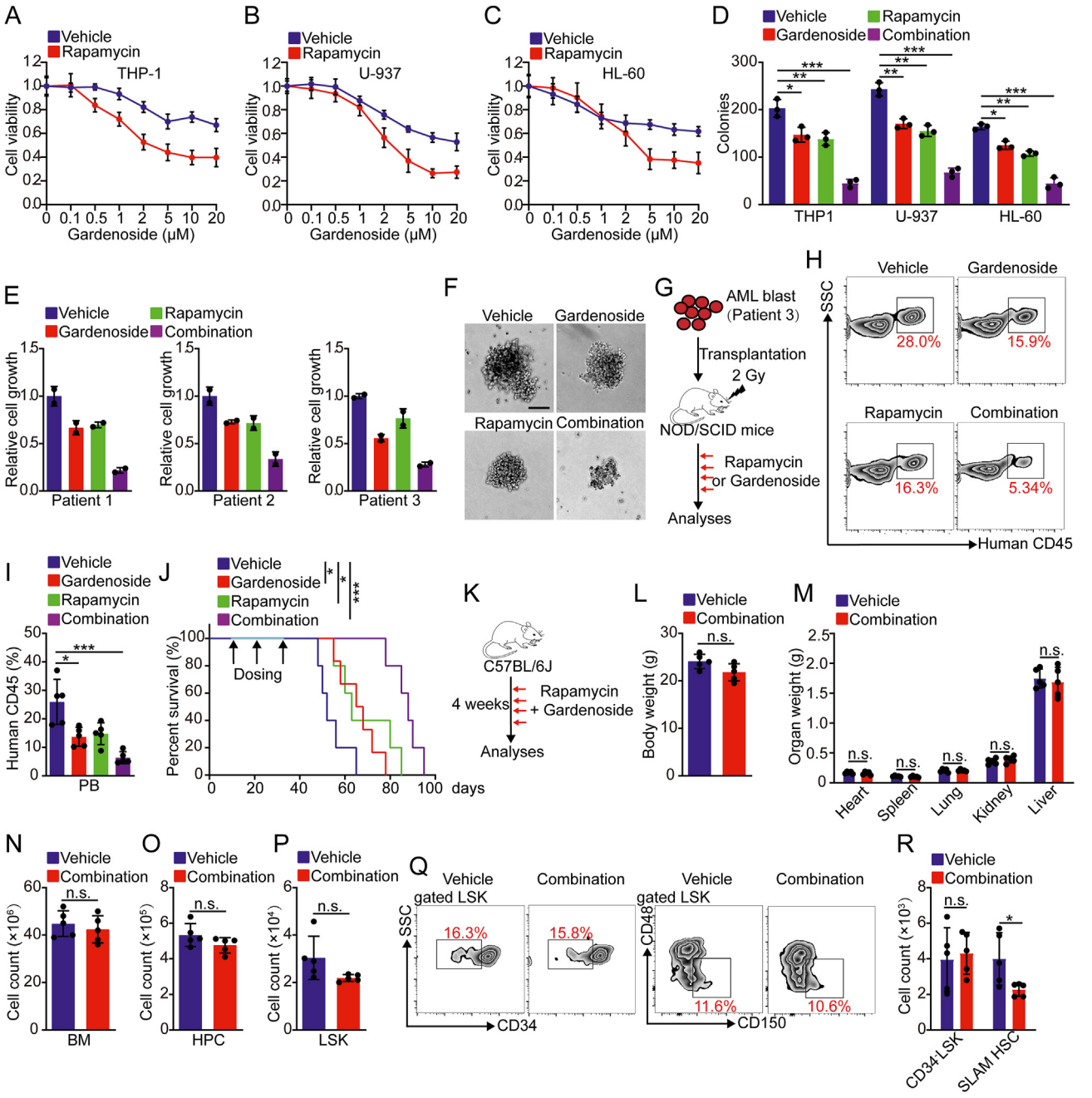

Figure 6 Gardenoside combined with rapamycin delays AML progression *in vivo*. **(A–C)** *In vitro* cell viability assay of leukemia cells using CCK8, with the treatment of vehicle or rapamycin (100 nM), along with different doses of Gardenoside for 48 h ($n = 4$). **(D)** Colony-forming assay of leukemia cells with the treatment of indicated inhibitors (rapamycin, 100 nM; Gardenoside, 5 μM; combination, rapamycin plus Gardenoside). The number of colonies was counted at 6–7 days after plating 5000 leukemia cells ($n = 3$). **(E)** *In vitro* proliferation assay of BM primary leukemia cells derived from AML patients using CCK8, with the treatment of indicated inhibitors for 48 h. **(F)** Representative images of colony-forming of BM leukemia cells derived from patient 3. Scale bar = 100 μm. **(G)** Experimental schematic for PDX. Patient 3-derived BM leukemia cells were transplanted into the NOD/SCID recipient mice. After 10 days of transplantation, NOD/SCID mice were treated with vehicle, Gardenoside (15 mg/kg, i. p. injection; three times a week), rapamycin (4 mg/kg, i. p. injection; three times a week), or a combination (Gardenoside plus rapamycin) for three weeks. **(H, I)** Flow cytometry analysis of human-CD45-positive leukemia cells in PB of recipient mice at the end of inhibitor treatment. The histograms indicate the percentages of $hCD45^+$ leukemia cells in PB ($n = 5$). **(J)** Kaplan-Meier survival of the mouse cohorts ($n = 5$ each) with indicated treatment. **(K)** Experimental schematic for the treatment of inhibitors. Wild-type C57BL/6 J were treated with vehicle, or Gardenoside (15 mg/kg, i. p. injection; three times a week) plus rapamycin (4 mg/kg, i. p. injection; three times a week) for 4 weeks. **(L, M)** The weight of the body and organs of mice with indicated inhibitor treatment. The weight was recorded at the end of treatment ($n = 5$). **(N)** Count of total BM cells in mice at the end of treatment ($n = 5$). **(O, P)** Count of HPC and LSK cells in BM of mice at the end of treatment ($n = 5$). **(Q)** Flow cytometry analysis of HSC ($CD34^-$LSK or $CD48^-CD150^+$LSK) in BM cells of mice at the end of treatment. **(R)**

findings, we demonstrated that the combinatorial inhibition of FOXO3A and mTOR resulted in a synergistic cytotoxic effect on AML cells and prolonged survival in a mouse model of AML. Moreover, we identified that Gardenoside was a potential FOXO3A inhibitor that exhibited anti-leukemia activity, and the combinatorial use of Gardenoside and rapamycin was a novel approach for AML intervention.

The intervention of AML largely relies on the understanding of molecular regulatory networks. Although several genes including *MLL*, *Myc*, *NOTCH*, and *β-catenin* have been uncovered to play critical roles in the expansion and myeloid differentiation of AML cells,[2,47] the molecular networks preserving AML cells remain largely unknown. Emerging evidence shows that *FOXO3A* is also a vital gene in AML progression. Highly phosphorylated FOXO3A and high FOXO3A expression are adverse prognostic factors in AML.[10,11] FOXO3A is required to preserve the immature state of AML cell lines and is essential for the progression of *MLL-AF9*-induced leukemia.[9] It has been revealed that the histone methyltransferase MLL4 positively regulates FOXO3A-dependent genes to inhibit myeloid maturation.[12] The gene expression array data showed about 78 dysregulated genes upon *FoxO1/3/4* deletion in murine LSK cells.[9] Ectopic *FoxO3a* expression reversed the expression of FoxOs-regulated genes (*e.g.*, *TSC22d3*, *Tek*, *Myl10*, *Gdpd3*, and *Col1a2*) in *MLL4*-deficient *MLL-AF9* leukemia cells.[12] However, whether the above-mentioned genes are direct targets of FOXO3A is unknown (lacking ChIP and rescue evidence); thus, how FOXO3A preserves AML cells remains obscure. Here, we utilized RNA-seq, CUT&Tag-seq, and ChIP-PCR to uncover multiple direct targets of FOXO3A, including *NOTCH3*, *CDKN2D*, *DNTT*, *CD70*, and *GNG7*. Our data showed that FOXO3A promoted the transcription of *NOTCH3*, which has been demonstrated to promote AML transformation and progression.[25] In contrast, we found that FOXO3A directly inhibited the transcription of *CDKN2D*, which is a well-known inhibitor for cell cycling via inducing G0/G1 phase arrest.[48] It has been revealed that CDKN2D suppresses the expansion of acute promyelocytic leukemia cells[26]; here, we demonstrated that the knockdown of *CDKN2D* substantially restored the colony-forming capacity of *FOXO3A*-deficient cells. Thus, through the molecular and functional experiments, we uncovered a unique context-dependent role of FOXO3A in preserving AML cells via its multiple targets.

mTOR is an evolutionally conserved kinase and has been found hyperactivated in AML patients.[27,28,49] Inhibition of mTOR (using rapamycin) suppresses expansion and induces apoptosis of AML, acute lymphoblastic leukemia, and chronic lymphocytic leukemia cells, indicating that leukemia cells require activated mTOR signaling to preserve proliferation and survival.[28,49,50] However, hyperactivated mTOR signaling drives leukemia stem cells (LSCs) to exit quiescence and eventually impairs LSC self-renewal,[51,52] suggesting the dual roles of mTOR in leukemia cells. mTOR forms two independent multiprotein-containing complexes, mTORC1, and mTORC2. mTORC2 can phosphorylate Akt, and the activated Akt directly inhibits FOXO3A via phosphorylation.[27,53] Inhibition of mTORC2 leads to a reactive activation of FOXO3A in leukemia cells, which protects leukemia cells from exhaustion.[54] FOXO3A is also reported to inhibit mTOR signaling via its transcriptional target TSC1 in hematopoietic FL5.12 cells,[34] suggesting an interplay between FOXO3A and mTOR signaling. Here, we discovered that FOXO3A restricted the activation of mTOR by inducing the expression of *GNG7*, which directly interacted with mTOR and inhibited the phosphorylation of mTOR. It seems that FOXO3A and mTOR mutually restrict each other, which may result in limited cytotoxicity on leukemia cells by single-target inhibition. Emerging evidence has demonstrated that combinatorial inhibition is a promising strategy for treating multiple cancers,[13] such as dual inhibition of KRAS and FGFR1 in lung cancer,[55] combinatorial anti-GD2 and anti-CD47 in neuroblastoma,[56] and synergistic inhibition of NOTCH and FLT3 in AML.[25] Here, we demonstrated that the combinatory inhibition of FOXO3A and mTOR efficiently killed AML cells and delayed AML progression *in vivo*, superior to single inhibition. However, whether there are more effective drug combinations to treat AML requires further screening.

Multiple transcription factors have been demonstrated to play pivotal roles in tumorigenesis and targeting transcription factors is a promising strategy for anticancer therapy.[2,47] Transcription factors have proved difficult to inhibit; regardless, several inhibitors have been developed. For instance, the small-molecule NSC59984 induces mutant p53 protein degradation via the ubiquitin-proteasome pathway.[57] The artepillin C disrupts the formation of the CREB/CRTC2 transcriptional complex which is a key regulator of hepatic gluconeogenesis.[58] Siomycin A inhibits the transcriptional activity of FOXOM1 and induces apoptosis of AML cells.[59] Through structure-based virtual screening, we reported a potential inhibitor of FOXO3A, Gardenoside, which is a natural compound extracted from the fruits of Gardenia. Gardenoside showed a strong capacity to inhibit FOXO3A DNA binding and impede the regulation of FOXO3A on its targets, *e.g.*, *CDKN2D*, *NOTCH3*, and *GNG7*, causing a substantial biological impact on AML cells. It has been reported that Gardenoside inhibits hepatocyte pyroptosis via the CTCF/DPP4 signaling,[60] as well as regulating the expression of P2X3 and P2X7 receptors in rats.[61] Although Gardenoside combined with rapamycin efficiently delayed AML progression and improved survival *in vivo*, it remains unknown whether Gardenoside regulates other factors and the target engagement of Gardenoside in leukemia cells requires further deep exploration. Moreover, Gardenoside only moderately inhibited the transcriptional activity of FOXO3A with IC50 values of 7.1 μM. Thus, further studies are warranted to optimize the FOXO3A inhibitors to improve their bioavailability, inhibitory effect, and therapeutic efficacy.

Overall, our results provided mechanistic evidence for the response of mTOR to FOXO3A inhibition in AML cells, revealing that mTOR inhibition enhanced the cytotoxic effect of *FOXO3A* depletion on AML cells. Moreover, we identified a potential FOXO3A inhibitor and demonstrated that Gardenoside combined with an mTOR inhibitor may be an effective therapeutic strategy for treating AML.

Count of $CD34^{-}$LSK and SLAM HSC ($CD48^{-}CD150^{+}$LSK) in BM cells of mice at the end of treatment. Error bars represent mean ± SD. $^{*}P < 0.05$, $^{**}P < 0.01$, $^{***}P < 0.001$; n. s., no significance; Student's *t*-test, one-way ANOVA, or Mantel-Cox test.

Author contributions

Y. Hou, J. Chen, and S. Xu conceived the project, analyzed data, and revised the paper. Z. Chen and Q. Guo performed experiments, analyzed data, and wrote the paper. L. Li, S. Huang, F. Wu, Z. Li, Z. Liu, and T. Chen performed some experiments. G. Song contributed to the data analysis and paper revision.

Conflict of interests

The authors have declared that no conflict of interests exists.

Funding

This work was supported by the Chongqing Science Fund for Distinguished Young Scholars, China (CSTB2022NSCQ-JQX0032), National Science Foundation of China (No. 81970100, 82170115 and 81700135), and the Doctor Research Project of Chongqing, China (No. CSTB2022BSXM-JCX0005).

Data availability

All sequencing data are deposited in the National Center for Biotechnology Information GEO database. RNA-seq and CUT&Tag data are available under accession no. GSE218289 and GSE218288. The datasets used and/or analyzed in our study are available from the corresponding author upon reasonable request.

Acknowledgements

We thank Dr. Renxiao Wang (School of Pharmacy, Fudan University) for technical aid in the molecular docking, visual screening, target fishing, and molecular dynamics simulation described in this work.

Appendix A. Supplementary data

Supplementary data to this article can be found online at https://doi.org/10.1016/j.gendis.2023.01.002.

References

1. Papaemmanuil E, Gerstung M, Bullinger L, et al. Genomic classification and prognosis in acute myeloid leukemia. *N Engl J Med*. 2016;374(23):2209—2221.
2. Yamashita M, Dellorusso PV, Olson OC, et al. Dysregulated haematopoietic stem cell behaviour in myeloid leukaemogenesis. *Nat Rev Cancer*. 2020;20(7):365—382.
3. Bowman RL, Busque L, Levine RL. Clonal hematopoiesis and evolution to hematopoietic malignancies. *Cell Stem Cell*. 2018;22(2):157—170.
4. Carter JL, Hege K, Yang J, et al. Targeting multiple signaling pathways: the new approach to acute myeloid leukemia therapy. *Signal Transduct Targeted Ther*. 2020;5(1):288.
5. Golson ML, Kaestner KH. Fox transcription factors: from development to disease. *Development*. 2016;143(24):4558—4570.
6. Hannenhalli S, Kaestner KH. The evolution of Fox genes and their role in development and disease. *Nat Rev Genet*. 2009;10(4):233—240.
7. Liu Y, Ao X, Ding W, et al. Critical role of FOXO3a in carcinogenesis. *Mol Cancer*. 2018;17(1):104.
8. Warr MR, Binnewies M, Flach J, et al. FOXO3A directs a protective autophagy program in haematopoietic stem cells. *Nature*. 2013;494(7437):323—327.
9. Sykes SM, Lane SW, Bullinger L, et al. AKT/FOXO signaling enforces reversible differentiation blockade in myeloid leukemias. *Cell*. 2011;146(5):697—708.
10. Santamaría CM, Chillón MC, García-Sanz R, et al. High *FOXO3a* expression is associated with a poorer prognosis in AML with normal cytogenetics. *Leuk Res*. 2009;33(12):1706—1709.
11. Kornblau SM, Singh N, Qiu Y, et al. Highly phosphorylated FOXO3A is an adverse prognostic factor in acute myeloid leukemia. *Clin Cancer Res*. 2010;16(6):1865—1874.
12. Santos MA, Faryabi RB, Ergen AV, et al. DNA-damage-induced differentiation of leukaemic cells as an anti-cancer barrier. *Nature*. 2014;514(7520):107—111.
13. Jaaks P, Coker EA, Vis DJ, et al. Effective drug combinations in breast, colon and pancreatic cancer cells. *Nature*. 2022;603(7899):166—173.
14. Bertram K, Leary PJ, Boudesco C, et al. Inhibitors of Bcl-2 and Bruton's tyrosine kinase synergize to abrogate diffuse large B-cell lymphoma growth *in vitro* and in orthotopic xenotransplantation models. *Leukemia*. 2022;36(4):1035—1047.
15. Wilson WH, Wright GW, Huang DW, et al. Effect of ibrutinib with R-CHOP chemotherapy in genetic subtypes of DLBCL. *Cancer Cell*. 2021;39(12):1643—1653.
16. He Y, Sun L, Xu Y, et al. Combined inhibition of PI3Kδ and FLT3 signaling exerts synergistic antitumor activity and overcomes acquired drug resistance in FLT3-activated acute myeloid leukemia. *Cancer Lett*. 2018;420:49—59.
17. Bruner JK, Ma HS, Li L, et al. Adaptation to TKI treatment reactivates ERK signaling in tyrosine kinase-driven leukemias and other malignancies. *Cancer Res*. 2017;77(20):5554—5563.
18. Jiang X, Mak PY, Mu H, et al. Disruption of Wnt/β-catenin exerts antileukemia activity and synergizes with FLT3 inhibition in *FLT3*-mutant acute myeloid leukemia. *Clin Cancer Res*. 2018;24(10):2417—2429.
19. Wang J, Li Y, Wang P, et al. Leukemogenic chromatin alterations promote AML leukemia stem cells via a KDM4C-ALKBH5-AXL signaling axis. *Cell Stem Cell*. 2020;27(1):81—97.e8.
20. Chen Z, Li L, Wu W, et al. Exercise protects proliferative muscle satellite cells against exhaustion via the Igfbp7-Akt-mTOR axis. *Theranostics*. 2020;10(14):6448—6466.
21. Chen Z, Huo D, Li L, et al. Nuclear DEK preserves hematopoietic stem cells potential via NCoR1/HDAC3-Akt1/2-mTOR axis. *J Exp Med*. 2021;218(5):e20201974.
22. Baell JB, Holloway GA. New substructure filters for removal of pan assay interference compounds (PAINS) from screening libraries and for their exclusion in bioassays. *J Med Chem*. 2010;53(7):2719—2740.
23. Friesner RA, Banks JL, Murphy RB, et al. Glide: a new approach for rapid, accurate docking and scoring. 1. Method and assessment of docking accuracy. *J Med Chem*. 2004;47(7):1739—1749.
24. van Galen P, Hovestadt V, Wadsworth II MH, et al. Single-cell RNA-seq reveals AML hierarchies relevant to disease progression and immunity. *Cell*. 2019;176(6):1265—1281.

25. Li D, Li T, Shang Z, et al. Combined inhibition of Notch and FLT3 produces synergistic cytotoxic effects in FLT3/ITD$^+$ acute myeloid leukemia. *Signal Transduct Targeted Ther*. 2020;5(1):21.
26. Wang Y, Jin W, Jia X, et al. Transcriptional repression of *CDKN2D* by PML/RARα contributes to the altered proliferation and differentiation block of acute promyelocytic leukemia cells. *Cell Death Dis*. 2014;5(10):e1431.
27. Bertacchini J, Heidari N, Mediani L, et al. Targeting PI3K/AKT/mTOR network for treatment of leukemia. *Cell Mol Life Sci*. 2015;72(12):2337—2347.
28. Beauchamp EM, Abedin SM, Radecki SG, et al. Identification and targeting of novel CDK9 complexes in acute myeloid leukemia. *Blood*. 2019;133(11):1171—1185.
29. Lin X, Fang Q, Chen S, et al. Heme oxygenase-1 suppresses the apoptosis of acute myeloid leukemia cells via the JNK/c-JUN signaling pathway. *Leuk Res*. 2015;39(5):544—552.
30. Zhang D, Zhou Q, Huang D, et al. ROS/JNK/c-Jun axis is involved in oridonin-induced caspase-dependent apoptosis in human colorectal cancer cells. *Biochem Biophys Res Commun*. 2019;513(3):594—601.
31. Wu JR, You RI, Hu CT, et al. Hydrogen peroxide inducible clone-5 sustains NADPH oxidase-dependent reactive oxygen species-c-Jun N-terminal kinase signaling in hepatocellular carcinoma. *Oncogenesis*. 2019;8(8):40.
32. Yilmaz OH, Valdez R, Theisen BK, et al. Pten dependence distinguishes haematopoietic stem cells from leukaemia-initiating cells. *Nature*. 2006;441(7092):475—482.
33. Bennett BL, Sasaki DT, Murray BW, et al. SP600125, an anthrapyrazolone inhibitor of Jun N-terminal kinase. *Proc Natl Acad Sci U S A*. 2001;98(24):13681—13686.
34. Khatri S, Yepiskoposyan H, Gallo CA, et al. FOXO3a regulates glycolysis via transcriptional control of tumor suppressor TSC1. *J Biol Chem*. 2010;285(21):15960—15965.
35. Chen CC, Jeon SM, Bhaskar PT, et al. FoxOs inhibit mTORC1 and activate Akt by inducing the expression of Sestrin3 and Rictor. *Dev Cell*. 2010;18(4):592—604.
36. Melick CH, Jewell JL. Regulation of mTORC1 by upstream stimuli. *Genes*. 2020;11(9):989.
37. Hartmann S, Szaumkessel M, Salaverria I, et al. Loss of protein expression and recurrent DNA hypermethylation of the *GNG7* gene in squamous cell carcinoma of the head and neck. *J Appl Genet*. 2012;53(2):167—174.
38. Shibata K, Tanaka S, Shiraishi T, et al. G-protein gamma 7 is down-regulated in cancers and associated with p 27kip1-induced growth arrest. *Cancer Res*. 1999;59(5):1096—1101.
39. Duc NM, Kim HR, Chung KY. Structural mechanism of G protein activation by G protein-coupled receptor. *Eur J Pharmacol*. 2015;763(Pt B):214—222.
40. Syrovatkina V, Alegre KO, Dey R, et al. Regulation, signaling, and physiological functions of G-proteins. *J Mol Biol*. 2016;428(19):3850—3868.
41. Liu J, Ji X, Li Z, et al. G protein γ subunit 7 induces autophagy and inhibits cell division. *Oncotarget*. 2016;7(17):24832—24847.
42. Lai WS, Ding YL. GNG7 silencing promotes the proliferation and differentiation of placental cytotrophoblasts in preeclampsia rats through activation of the mTOR signaling pathway. *Int J Mol Med*. 2019;43(5):1939—1950.
43. Lai W, Yu L. Elevated microRNA 183 impairs trophoblast migration and invasiveness by downregulating FOXP1 expression and elevating GNG7 expression during preeclampsia. *Mol Cell Biol*. 2020;41(1):e00236-20.
44. Obrist D, Nienhaus A, Zamaro E, et al. Determinants for a successful Sémont maneuver: an *In vitro* study with a semicircular canal model. *Front Neurol*. 2016;7:150.
45. Tsai KL, Sun YJ, Huang CY, et al. Crystal structure of the human FOXO3a-DBD/DNA complex suggests the effects of post-translational modification. *Nucleic Acids Res*. 2007;35(20):6984—6994.
46. Liang H, Zhang L, Wang H, et al. Inhibitory effect of gardenoside on free fatty acid-induced steatosis in HepG2 hepatocytes. *Int J Mol Sci*. 2015;16(11):27749—27756.
47. Verovskaya EV, Dellorusso PV, Passegué E. Losing sense of self and surroundings: hematopoietic stem cell aging and leukemic transformation. *Trends Mol Med*. 2019;25(6):494—515.
48. Han X, Kuang Y, Chen H, et al. p19INK4d: More than just a cyclin-dependent kinase inhibitor. *Curr Drug Targets*. 2020;21(1):96—102.
49. Dai YJ, Wang YY, Huang JY, et al. Conditional knockin of Dnmt3a R878H initiates acute myeloid leukemia with mTOR pathway involvement. *Proc Natl Acad Sci U S A*. 2017;114(20):5237—5242.
50. Ge Z, Song C, Ding Y, et al. Dual targeting of MTOR as a novel therapeutic approach for high-risk B-cell acute lymphoblastic leukemia. *Leukemia*. 2021;35(5):1267—1278.
51. Lechman ER, Gentner B, Ng SWK, et al. miR-126 regulates distinct self-renewal outcomes in normal and malignant hematopoietic stem cells. *Cancer Cell*. 2016;29(2):214—228.
52. Hoshii T, Tadokoro Y, Naka K, et al. mTORC1 is essential for leukemia propagation but not stem cell self-renewal. *J Clin Invest*. 2012;122(6):2114—2129.
53. Fu Z, Tindall DJ. FOXOs, cancer and regulation of apoptosis. *Oncogene*. 2008;27(16):2312—2319.
54. Fang Y, Yang Y, Hua C, et al. Rictor has a pivotal role in maintaining quiescence as well as stemness of leukemia stem cells in MLL-driven leukemia. *Leukemia*. 2017;31(2):414—422.
55. Manchado E, Weissmueller S, Morris 4th JP, et al. A combinatorial strategy for treating KRAS-mutant lung cancer. *Nature*. 2016;534(7609):647—651.
56. Theruvath J, Menard M, Smith BAH, et al. Anti-GD2 synergizes with CD47 blockade to mediate tumor eradication. *Nat Med*. 2022;28(2):333—344.
57. Zhang S, Zhou L, Hong B, et al. Small-molecule NSC59984 restores p53 pathway signaling and antitumor effects against colorectal cancer via p73 activation and degradation of mutant p53. *Cancer Res*. 2015;75(18):3842—3852.
58. Chen Y, Wang J, Wang Y, et al. A propolis-derived small molecule ameliorates metabolic syndrome in obese mice by targeting the CREB/CRTC2 transcriptional complex. *Nat Commun*. 2022;13(1):246.
59. Sheng Y, Yu C, Liu Y, et al. FOXM1 regulates leukemia stem cell quiescence and survival in MLL-rearranged AML. *Nat Commun*. 2020;11(1):928.
60. Shen T, Lei T, Chen L, et al. Gardenoside hinders caspase-1-mediated hepatocyte pyroptosis through the CTCF/DPP4 signaling pathway. *Front Physiol*. 2021;12:669202.
61. Yu M, Su B, Zhang X. Gardenoside suppresses the pain in rats model of chronic constriction injury by regulating the P2X3 and P2X7 receptors. *J Recept Signal Transduction*. 2018;38(3):198—203.